International Journal of Mathematics, Statistics and Operations Research
Vol. 2; Number 2; 2022, pp. 163-186
https://doi.org/10.47509/IJMSOR.2022.v02i02.05

ARF INDIA
Academic Open Access Publishing
www.arfjournals.com

Numerical Simulation of Gas-Solid Flow in CFB Riser Using Different Approaches of Kinetic Theory of Granular Flows

Renato César da Silva,* Luben Cabezas-Gómez,† Hélio Aparecido Navarro‡

August 3, 2022

Abstract

In this paper is applied the two-fluid model to simulate the gas-solid flow in a riser of a circulating fluidized bed (CFB). The phases are modeled as a continuum medium computing the solid's pressure and dynamic viscosity by the kinetic theory of granular flows (KTGF). The numerical simulations are performed with the MFIX (Multiphase Flow with Interface eXchanges) computational fluid dynamics (CFD) code developed in the National Energy Technology Laboratory (NETL). The main aim of this work is to perform a comparative analysis of the simulation results obtained from three different versions of the KTGF. In the work are presented time-averaged results comprehending the radial profiles of the axial velocities of gas and solid phases, the solid volumetric fraction and the solid mass flow. These results are compared with the available experimental data showing a different behavior for each version of the KTGF. For a more complete comparative analysis also are presented time-averaged and transient snapshots of the gas volumetric fraction in two risers sections disposed at two different heights of the column. In all the simulations is used a uniform two-dimensional computational mesh and the Superbee second order scheme for the discretization of the advective terms. The numerical results show that the procedure for the computation of the solid phase pressure and viscosity influences in a significant way the behavior of the gas-solid flow in a riser. These differences are

*Associate Professor, Department of Mathematics, Federal University of Mato Grosso do Sul. Email id: renato.silva@ufms.br, ORCID: 0000-0002-7931-7785.

†Associate Professor, Mechanical Engineering Department, Sao Carlos School of Engineering, University of Sao Paulo. Email id: lubencg@sc.usp.br, ORCID: 0000-0002-9550-9453.

‡Associate Professor, Mechanical Engineering Department, Sao Carlos School of Engineering, University of Sao Paulo. (*in memorian*)

Article History
Received : 3 August 2022; Revised : 29 August 2022; Accepted : 19 September 2022; Published : 29 December 2022

To cite this paper

Renato César da Silva, Luben Cabezas-Gomez, Helio Aparecido Navarro (2022). Numerical Simulation of Gas-Solid Flow in CFB Riser using Different Approaches of Kinetic Theory of Granular Flows. *International Journal of Mathematics, Statistics and Operations Research.* 2(2), 163-186.

obtained even when it is considered only the KTGF with slightly variations for the constitutive equations computations.

Keywords: Gas-solids flows, circulating fluidized beds, kinetic theory of granular flows, numerical simulation, MFIX code.

1 Introduction

In this work are presented numerical simulation results for the gas-solid two-phase flow in a CFB riser. The results were obtained using the MFIX code, Syamlal et al. (1993) and considering three different versions of the KTGF. In hydrodynamics simulations of gas-solid flows it is a common issue to consider the participating phases as a continuum medium and to consider two different main procedures for the calculation of the dispersed solid-phase constitutive equations (mainly the solid pressure and first and second viscosity coefficients). These procedures are the so-called traditional procedure, which rely on the use of empirical correlations obtained from experiments, c.f., Gidaspow (1994), Huilin and Gidaspow (2003), Cabezas-Gómez and Milioli (2003), Cabezas-Gómez and Milioli (2005), Cabezas-Gómez et al (2008), and the KTGF, which uses theoretical relations for computation of the solid phase constitutive relations parameters (see the works cited in the review below). The KTGF have been used considering mainly two versions, the algebraic version Syamlal et al. (1993), Guenther and Syamlal (2001), Syamlal and O'Brien (2004) e Cabezas-Gómez et al. (2006) where the granular temperature is computed solving algebraic equations, and other more sophisticated version where the granular temperature is computed solving a partial differential equation (PDE) representing the granular kinetic energy balance Neri and Gidaspow (2000), Agrawal et al. (2001), Benyahia et al. (2000), among others.

In the present work besides the above two KTGF models (namely the algebraic version and that which solves the PDE for computation of granular temperature) it is also used a modified version of the algebraic KTGF model for numerical simulations, here named as the hybrid model. The balance equations for these models are introduced in section 2. Now a brief introduction of the models is presented. The KTGF bases on the similarities between flow of a granular material, which comprehends a particles population with or without an interstitial gas, and the molecules of a gas. This treatment uses the classical results of kinetic theory for dense gases introduced in Chapman and Cowling (1961 and 1970). According to Gidaspow (1994), it is believed that in 1954 Bagnold (1954) was the pioneer in the use of the KTGF.

Of the works concerning to the KTGF development can highlight the next: Jenkins and Savage (1983), Savage (1983), Lun et al. (1984), and Jenkins and

Richman (1985). These works served as starting point for the development and industrial application of the KTGF to multiphase gas-solid flows, mainly in gas-solid fluidization processes, such as those studied by Sinclair and Jackson (1989), Ding and Gidaspow (1990), Kim and Arastoopour (1995), and Boemer et al. (1995), among others. One of the more complete analyses developed with the two-fluid model using the KTGF has been accomplished by the Electricité de France (EDF) group (Peirano (1998)).

An algebraic version of the KTGF was developed by Syamlal et al. (1993), bringing the possibility of convergence acceleration by directly computing the granular temperature from a simple algebraic expression instead of solving a complex partial differential equation (PDE) for the conservation of granular energy. The most notable difference between the algebraic and other versions of KTGF is the use of a simplified balance equation for the granular temperature calculation. In this procedure both convection and diffusion processes are neglected, and only local stationary dissipation of granular energy is taken into account. From the computed granular temperature, and applying theoretical relations developed by Lun et al. (1984), solids phase pressure and viscosities are determined. According to van Wachem et al. (1998) following Syamlal et al. (1993), this procedure is valid only for higher values of the solids volumetric fraction and relatively low values of solids velocity. In such a regime the kinetic granular is mostly dissipated locally. The approach is more appropriate for gas-solids flows in bubbling fluidized beds (BFB). However, following the literature, the procedure is used in the present work to simulate the gas-solid flow in a CFB riser.

The modified version of the algebraic KTGF (hybrid model) uses the model developed by Syamlal et al. (1993) slightly changed. In this new model the solid phase dynamic viscosity is computed by the algebraic version of KTGF, while the solid pressure is calculated applying empirical correlations of the two-fluid model traditional procedure. The correlations are function of an elasticity modulus accounting for collisional interactions among particles, c.f. Gidaspow (1994). Thus, the modified procedure can be considered a hybrid procedure mixing up elements of both the traditional and algebraic KTGF procedures. The present results show that this hybrid model provides qualitatively acceptable predictions, even better than the algebraic version of the KTGF, at least, in relation to the experimental data used for comparison. Some initial results with this model were published in Cabezas-Gómez et al. (2006).

The main aim of this work is to perform a comparative analysis of the simulation results obtained with the different three procedures for the determination of solid phase pressure and viscosity above commented, namely, the algebraic KTGF, the hybrid approach and the KTGF solving the PDE for granular temperature computation. For this purpose these three models are denoted in the paper as 'model 1', 'model 2' and 'model 3', respectively. All the numerical simulations

were performed for the CFB installation described in Luo (1987), considering the Superbee scheme (Sweby, (1984)) for the discretization of the advective terms of balance equations. Nowadays, works considering an Eulerian-Lagrangian modeling approaches are used for simulating the problems studied in this paper, i.e., see Caserta et al. (2016).

2 Mathematical formulation

The mathematical models are based on the mathematical construction of interpenetrating continuous phases. For this purpose some kind of averaged technique should be performed to average the local temporal variables over a region that is large compared to the particles spacing but sufficient small than the flow domain. A temporal average also is constructed considering a small time interval for constructing the time-averaged quantities, which remain instantaneous for high temporal scales. Detailed descriptions used to obtain gas-solid multiphase mathematical models considering different averaged procedures are presented in Anderson and Jackson (1967), Soo (1967), Drew (1983), Gidaspow (1994), Enwald et al. (1996).

The equations solved by the MFIX code used in this work are those given in Syamlal et al. (1993) and Benyahia et al. (2006). In the present study is used the hydrodynamic model B, developed at IIT (Illinois Institute of Technology) (see Gidaspow (1994)). The following hypotheses are considered: both phases are assumed to be isothermal at 300K; no interface mass transfer is assumed; the solid phase is characterized by a mean particle diameter, density and sphericity factor; both phases are continuous assuming a single gas phase (air) and a single solid phase (glass beads). Next is presented the system of governing equations used in the three mathematical models used in numerical simulations. The models only have differences in the solid phase stress tensor computation, the other equations applied for each model. The continuity equations, representing the mass conservation for gas and solid phases, respectively, are written as:

$$\frac{\partial(\rho_g \alpha_g)}{\partial t} + \nabla.(\rho_g \alpha_g v_g) = 0 \tag{1}$$

$$\frac{\partial(\rho_s \alpha_s)}{\partial t} + \nabla.(\rho_s \alpha_s v_s) = 0 \tag{2}$$

where v_g and v_s represent the velocities (m/s), ρ_g and ρ_s the densities (kg/m^3) and α_g and α_s stand for the volumetric fractions of gas and solid phases, respectively. By definition the following relation applies for the volumetric fractions:

$$\alpha_g + \alpha_s = 1 \tag{3}$$

The momentum equation for the gas phase is expressed as:

$$\frac{\partial(\rho_g \alpha_g v_g)}{\partial t} + \nabla.(\rho_g \alpha_g v_g v_g) = -\nabla P + \nabla.(\alpha_g \tau_g) - \beta_B (v_g - v_s) + \rho_g g \quad (4)$$

To model the constitutive equations for the gas phase it is assumed a Newtonian fluid and the Stokes hypothesis. The following relation holds for the viscous stress tensor, τ_g:

$$\tau_g = \mu_g \left[\nabla v_g + (\nabla v_g)^T - \frac{2}{3}(\nabla . v_g)\bar{\bar{I}} \right] \quad (5)$$

In the Eq. (4) g represents the gravity acceleration (m/s^2), P represents the thermodynamic gas pressure (Pa), and β stands for the stationary drag function at interface between the gas and solid phase (kg/(m^2.s)). The subscript B represents the hydrodynamic model B. In this model the gas pressure gradient term it is not present in the solid phase momentum equation and the drag function is modified to satisfy the Archimedes' principle and the usual relation for the minimum fluidization Gidaspow (1994). In Eq. (5) μ_g is the dynamic viscosity being assumed constant and equal to $1.8\text{x}10^{-5}$ (kg/(m.s)) and $\bar{\bar{I}}$ is a unit tensor.

The drag function is used to compute the stationary drag force at the interface. This force represents the momentum transfer between the gas and solid phases. The drag function is computed considering the procedure of Gidaspow (1994) and coworkers, where Ergun (1965) correlation is used for $\alpha_s \geq 0.2$ and Wen and Yu (1966) correlation is used for $\alpha_s < 0.2$, respectively.

The drag function for $\alpha_s \geq 0.2$:

$$\beta = 150\frac{\alpha_s^2 \mu_g}{\alpha_g^2 (d_p \Phi_s)^2} + 1.75\frac{\rho_g \alpha_s |v_g - v_s|}{(\alpha_g d_p \Phi_s)} \quad (6)$$

and for $\alpha_s < 0.2$:

$$\beta = \frac{3}{4} C_{Ds} \frac{\rho_g \alpha_s |v_g - v_s|}{d_p \Phi_s} \alpha_g^{-2.65} \quad (7)$$

In relation (7) C_{Ds} represents the interface drag coefficient for a single particle in an infinite medium, calculated by:

$$C_{Ds} = \begin{cases} \frac{24}{Re_s}\left(1 + 0.15.Re_s^{0.687}\right) & for\ \ Re_s < 1000 \\ 0.44 \quad for \quad Re_s \geq 1000 \end{cases} \quad (8)$$

The Reynolds number, Re_s is based on the particle mean diameter, d_p (m) and considers the particle sphericity, Φ_s equals to unity in the present study:

$$Re_s = \frac{\alpha_g \rho_g |v_g - v_s| d_p \Phi_s}{\mu_g} \quad (9)$$

The momentum equation for the solid phase is expressed as:

$$\frac{\partial(\rho_s \alpha_s v_s)}{\partial t} + \nabla.(\rho_s \alpha_s v_s v_s) = \nabla.S_s + \beta_B (v_g - v_s) + (\rho_s - \rho_g)\alpha_s g \quad (10)$$

In Eq. (10), S_s represents the stress tensor for the solid phase being defined by combination of theories for viscous and plastic flow regimes according to Syamlal et al. (1993) as:

$$S_s = \begin{cases} -P_s^p \bar{\bar{I}} + \tau_s^p, \ if \ \alpha_g \leq \alpha_g^* \\ -P_s^v \bar{\bar{I}} + \tau_s^v, \ if \ \alpha_g > \alpha_g^* \end{cases} \quad (11)$$

where P_s stands for the solid pressure (Pa) and τ_s for the viscous solid stresses (Pa), respectively. The superscripts p is used for the plastic regime and v for the viscous regime. The variable α_g^* is equal to the void fraction at the minimum fluidization. The variations in the present models concern only to the formulation of the solid viscous stresses in the viscous regime. In the plastic regime all models use the same formulation. The plastic stresses are calculated using the Schaeffer's (1987) formulation as:

$$\tau_s^p = 2\mu_s^p D_s \quad (12)$$

where

$$\mu_s^p = \frac{P^* sin(\Phi)}{2\sqrt{I_{2D}}} \quad (13)$$

In relations (12) and (13) D_s represent the strain rate tensor of the solid phase, I_{2D} is the second invariant of the deviator of the strain rate tensor and Φ is an angle of internal friction, assumed equal to zero (c.f. Syamlal et al. (1993)). The first two parameters as computed as:

$$I_{2D} = \frac{1}{6}\left[(D_{s_{11}} - D_{s_{22}})^2 + (D_{s_{22}} - D_{s_{33}})^2 + (D_{s_{33}} - D_{s_{11}})^2\right] + D_{s_{12}}^2 + D_{s_{23}}^2 + D_{s_{31}}^2 \quad (14)$$

$$D_s = \frac{1}{2}\left(\nabla v_s + (\nabla v_s)^T\right) \quad (15)$$

Similar to the functions typically used in plastic flow theories (Jenike (1987)), an arbitrary function that allows a certain amount of compressibility in the solid phase represent the solid pressure term in the plastic flow regime:

$$P_s^p = \alpha_s P^* \quad (16)$$

where P^* is represented by an empirical law according to Jenike (1987):

$$P^* = 10^{25}\left(\alpha_g^* - \alpha_g\right) \quad (17)$$

The three considered models in the paper only differ in the formulation of the stress tensor in the viscous regime. Nevertheless, for all the models the viscous solid stress in the viscous regime is formulated as:

$$\tau_s^v = 2\mu_s^v D_s + \lambda_s^v tr\left(D_s\right)\bar{\bar{I}} \tag{18}$$

The differences are related mainly to the computation of the first, μ_s, and second, λ_s, viscosity coefficients of the solid phase (dynamic and volumetric viscosities, respectively). Also the formulation of the solid pressure, P_s, differs slightly. The first model is the algebraic version of the KTGF. For this model the following relations apply (Syamlal (1993)). The granular temperature, θ, $\left(m^2/s^2\right)$ is computed by an algebraic version of the balance equation for granular temperature obtained by Lun et al. (1984). This algebraic equation is obtained assuming that the granular temperature is dissipated locally, neglecting the diffusion and convective terms and retaining only the dissipative and font terms (Syamlal (1993)):

$$\Theta = \left(\frac{-K_1\alpha_s tr\left(D_s\right) + \sqrt{K_1^2\alpha_s^2 tr^2\left(D_s\right) + 4K_4\alpha_s\left(K_2 tr^2\left(D_s\right) + 2K_3 tr\left(D_s^2\right)\right)}}{2\alpha_s K_4} \right) \tag{19}$$

To compute the granular temperature from the above relation the following constant functions are used:

$$K_1 = 2\left(1+e\right)\rho_s g_0 \tag{20}$$

$$K_2 = \frac{4}{3\sqrt{\pi}} d_p \rho_s \left(1+e\right)\alpha_s g_0 - \frac{2}{3}K_3 \tag{21}$$

$$K_3 = \frac{d_p\rho_s\sqrt{\pi}}{6\left(3-e\right)}\left[1+\frac{2}{5}\left(1+e\right)\left(3e-1\right)\alpha_s g_0\right] + \frac{8 d_p \rho_s \alpha_s g_0 \left(1+e\right)}{10\sqrt{\pi}} \tag{22}$$

$$K_4 = \frac{12\left(1-e^2\right)\rho_s g_0}{d_p\sqrt{\pi}} \tag{23}$$

In the above relations, Eq. (20-23), g_0 stands for the radial distribution function at contact of particles calculated by the correlation of Carnahan and Starling (1969):

$$g_0 = \frac{1}{\alpha_g} + \frac{1.5\alpha_s}{\alpha_g^2} + \frac{0.5\alpha_s^2}{\alpha_g^3} \tag{24}$$

After the computation of all the necessary parameters the dynamic and volumetric solid viscosities are computed respectively by the Eqs. (25) and (26) below:

$$\mu_s^v = K_3\alpha_s\sqrt{\Theta} \tag{25}$$

$$\lambda_s^v = K_2 \alpha_s \sqrt{\Theta} \tag{26}$$

For the algebraic version of KTGF, the denominated "model 1" in the present work, the solid phase granular pressure is expressed as (Syamlal (1993)):

$$P_s^v = K_1 \alpha_s^2 \Theta \tag{27}$$

This model only considers the particle collisions' contribution to the granular solids pressure property. This term accounts for the momentum transfer by direct collisions. The formulation of "model 2", described here as a hybrid model, considers the same equations of the algebraic version of the KTGF, presented above, excepting the formulation of the granular solid pressure term. This term is formulated considering the traditional two-fluid modeling approach where the solid phase pressure is modeled empirically using the solid elastic modulus, G, in $\left(N/m^2\right)$ as:

$$P_s^v = G \nabla \alpha_s \tag{28}$$

The solid elasticity modulus is a function of the void fraction computed by the correlation of Gidaspow and Ettehadieh (1983):

$$G(\alpha_g) = 10^{-8.76\alpha_g + 5.43} \ \left(Pa/m^2\right) \tag{29}$$

This approach considers only the solid pressure gradient due to particle collisions. In the traditional procedure the kinetic influence is commonly neglected (Enwald et al. (1996)).

The third model, "model 3", is the KTGF that solves a partial differential equation for computing the granular temperature. In this case is used the Princeton model Agrawal et al (2001), described in details in Benyahia et al. (2006) and fully implemented in the MFIX code.

The pseudo-thermal energy PTE balance for computing the granular temperature is expressed as:

$$\left[\frac{\partial\left(\frac{3}{2}\alpha_s \rho_s \Theta\right)}{\partial t} + \nabla.\left(\frac{3}{2}\alpha_s \rho_s v_s \Theta\right)\right] = -\nabla.\mathbf{q} - \mathbf{S_s} : \nabla \mathbf{v_s} + \Gamma_{\mathbf{slip}} - \mathbf{J_{coll}} - \mathbf{J_{vis}} \tag{30}$$

The first term of the right hand side of this equation represent the diffusive transport of PTE, with q representing the diffusive flux of kinetic granular energy. The second and third terms represent rates of production of kinetic granular energy by shear (viscous regime) and gas-particle slip, respectively. The fourth and fifth terms denote rates of dissipation of PTE through inelastic collisions and viscous damping, respectively (Agrawal et al. (2001)).

The rates of production of PTE by gas-slip, and of dissipation of PTE through inelastic collisions and viscous damping are respectively expressed as:

$$\Gamma_{slip} = \frac{81\alpha_s\mu_g^2\left|v_g - v_s\right|}{g_0 d_p^3 \rho_s \sqrt{\pi\Theta}} \tag{31}$$

$$J_{coll} = \frac{48}{\sqrt{\pi}}\eta\left(1-\eta\right)\frac{\rho_s\alpha_s^2}{d_p}g_0\Theta^{3/2} \tag{32}$$

$$J_{vis} = 3\beta\Theta \tag{33}$$

The solid phase stresses in the viscous regime are formulated as:

$$S_s = P_s^v\bar{\bar{I}} - \tau_s^v = P_s^v\bar{\bar{I}} - \lambda_s^v\left(\nabla.v_s\right)\bar{\bar{I}} + 2\mu_s^v\left[D_s - \frac{1}{3}\left(\nabla.v_s\right)\bar{\bar{I}}\right] \tag{34}$$

In relation (34) the solid pressure and the volumetric and dynamic viscosities are expressed as:

$$P_s^v = \alpha_s\rho_s\left(1+4\eta\alpha_s g_0\right)\Theta \tag{35}$$

$$\lambda_s^v = \eta\mu_b \tag{36}$$

$$\mu_s^v = -\left(\frac{2+\alpha}{3}\right)\left\{\frac{2\mu^*}{g_0\eta\left(2-\eta\right)}\left(1+\frac{5}{8}\alpha_s g_0\right)\left(1+\frac{5}{8}\eta\left(3\eta-2\right)\alpha_s g_0\right)+\frac{6}{5}\eta\mu_b\right\} \tag{37}$$

where

$$\mu_b = \frac{256\mu\alpha_s^2 g_0}{5\pi} \tag{38}$$

$$\mu = \frac{5\rho_s d_p\sqrt{\pi\Theta}}{96} \tag{39}$$

$$\mu^* = \frac{\mu}{1+\frac{2\beta\mu}{\left(\rho_s\alpha_s\right)^2 g_0\Theta}} \tag{40}$$

$$\eta = \frac{\left(1+e\right)}{2} \tag{41}$$

$$\alpha = 1.6 \tag{42}$$

e represents the particle-particle collision restitution coefficient. In the present work e is equal to 0.8.

The diffusive flux of PTE is formulated as:

$$\mathbf{q} = -k_s^v\nabla\Theta \tag{43}$$

In Eq. (43) the conductivity of the granular solid phase is expressed as:

$$k_s^v = -\frac{\lambda^*}{g_0}\left\{\left(1+\frac{12}{5}\eta^2(4\eta-3)\alpha_s g_0\right)+\frac{64}{25\pi}(41-33\eta)\eta^2\alpha_s^2 g_0^2\right\} \tag{44}$$

where

$$\lambda^* = \frac{\lambda}{1+\frac{6\beta\lambda}{5(\rho_s\alpha_s)^2 g_0\Theta}} \tag{45}$$

and

$$\lambda = \frac{75\rho_s d_p\sqrt{\pi\Theta}}{48\eta(41-33\eta)} \tag{46}$$

It should be noted that the solid-phase stress in the viscous regime, as well as, the PTE diffusive flux are expressed in a manner very similar to that proposed in Lun et al. (1984), see Eqs. (34) – (46). To account for the role of the interstitial fluid Agrawal et al. (2001) included in these expressions the terms μ^* and λ^*. This work should be consulted for more details on Princeton model.

Finally, the fluidization medium, air, is modeled as an ideal fluid by the ideal gas state equation:

$$\rho_g = \frac{P}{(R_g T)} \tag{47}$$

In Eq. (47), R_g is the ideal gas constant (kJ/kg-K). In all equations the subscripts (g) and (s) respectively stand for gas and solid phases and t is the time (s).

3 Geometry and simulation conditions

In the simulations was employed a two-dimensional computational domain applying a Cartesian coordinate system. The geometric dimensions are those specified in Cabezas-Gómez and Milioli (2003) and Cabezas-Gómez and Milioli (2005). The riser height is equal to 5.5762 meters and a diameter equal to 0.0762 meters. The inlet section is located at 0 meter height and has a dimension equal to the riser diameter. The exit section is located at the right wall after 5.5 meters height.

For simulation the following data were assumed: mean solid particle diameter, d_p = 520 μm; solid phase density, ρ_s = 2,620 kg/m^3; mean solid mass flux, G_s = 24.9 kg/(m^2 - s); and molecular gas phase viscosity equal to, μ_g = 1.8x10^{-5} Pa.s.

For first temporal integration the assumed riser initial conditions are: riser without solids, α_s = 0; gas pressure equal to P = 101.325 kPa and gas temperature T = 300 K. It should be noted that the gas-solid flow is isothermal.

The formulation of boundary conditions is of great importance for the quality of the numerical results. In the present problem are formulated boundary conditions at the inlet and outlet riser's sections, as well as, at the riser walls. At the riser inlet is assumed a constant solid mass flow, defining the gas and solid phase normal velocities and the solid volumetric fraction as: $v_s = 0.386$ m/s, $v_g = 4.979$ m/s and $\alpha_s = 0.0246$. The MFIX need the inlet setting of gas pressure and temperature taken equal to P = 120.6639 kPa and T = 300 K. To close the necessary BCs at the inlet region is assigned a constant inlet value for the granular temperature. In this case this parameter was assumed to be equal to $\theta = 0.1\ m^2/s^2$.

At the riser outlet it is assumed a developed flow applying the following condition in the normal direction to the outlet region:

$$\frac{\partial f}{\partial \mathbf{n}} = 0 \tag{48}$$

where f is α_g, u_g and u_s. The gas pressure is fixed to P = 117.2049 kPa. The above relations apply for all the mathematical models.

The differences are found in the formulation of BCs at riser's walls. At the walls it is considered for the gas phase a no slip boundary condition for the three models. For the solid phase it is assumed a partial slip boundary condition (Ding and Gidaspow (1990)) in the tangential direction to the wall according to Eq. (49) for the models 1 and 2, respectively. This equation was implemented in the MFIX code by the authors.

$$v_{s,w} = -\frac{d_p}{\alpha_s^{1/3}} \frac{\partial v_s}{\partial \mathbf{n}} \tag{49}$$

For model 3 a partial slip boundary condition for tangential solid velocity and granular temperature according to Johnson and Jackson (1987) are applied. These equations are implemented in the default version of the MFIX code and are represented by the Eqs. (50) and (51).

$$\mathbf{n}.\mathbf{S_s}.\mathbf{t} + \frac{\pi}{2\sqrt{3}\alpha_{smax}} \Phi' \rho_s \alpha_s g_0 \Theta^{\frac{1}{2}} v_{slip} = 0 \tag{50}$$

$$\mathbf{n}.\mathbf{q} = \frac{\pi\sqrt{3}}{6\alpha_{smax}} \Phi' \rho_s \alpha_s g_0 \Theta^{\frac{1}{2}} |v_{sl}| - \frac{\pi\sqrt{3}}{4\alpha_{smax}} \left(1 - e_w^2\right) \rho_s \alpha_s g_0 \Theta^{\frac{3}{2}} \tag{51}$$

where the slip velocity at the wall is computed by:

$$v_{sl} = v - v_w \tag{52}$$

In Eqs. (50) and (51), e_w represents the particle-wall restitution coefficient, ϕ' stands for specularity coefficient and **n** represent a unitary normal vector. The first two variables assume the following MFIX default values: e_w = 1.0 and ϕ' = 0.6,

respectively. A additional discussion about boundary condition effects on CFB disperse gas-solid flow in presented in Benyahia et al. (2005).

In the normal direction to the wall it is considered a no slip condition for both phases. For pressure and solid volumetric fraction a free slip boundary condition was applied, assuming a null gradient normal to the wall of each variable.

In this work is used a Cartesian coordinate system considering uniform computational mesh in radial direction with 22 cells (δ_x = 0.381 cm) and uniform in axial direction with 148 cells (δ_y = 3.81 cm) totalizing a number of 2920 cells in the whole domain. An appropriateness of using this computational mesh for gas-solid flows simulation is discussed in Cabezas-Gómez et al (2008). The simulations with all models are performed for t = 100 seconds of fluidization.

4 Numerical results and discussion

The numerical simulations were developed using the MFIX code (Syamlal et al (1993)). This numerical code is widely used for the simulation of multiphase gas-solid flows (Guenther and Syamlal (2001), Syamlal and O'Brien (2003), Cabezas-Gómez et al. (2006), Benyahia et al. (2005), Benyahia et al. (2006), beside others). The above three mathematical models are all available in the MIFX code. The authors implemented the solid pressure correlation from the traditional procedure (see Eqs. 28 and 29) used in model 2, along with the partial slip solid phase BC at the walls (Eq. 49).

Next are presented the simulation results obtained with the three mathematical models. The model 1 stands for the algebraic version of the KTGF, the model 2 represents the results obtained with the hybrid approach, and the results obtained with the KTGF, solving a PDE for granular temperature computation are denoted by the model 3. The hybrid model can be considered as an "ad-hoc" model proposition, leading to interesting results.

In Figures 1 – 4 are shown the numerical results analyzed in the paper for which are disposable experimental data. In all these figures are displayed mean time profiles obtained for a temporal interval of 80 seconds, taken from 20 up to 100 seconds of simulation.

In Figure 1 are observed the radial profiles of the mean time solid volumetric fraction at 3.4 meters above the riser inlet for the three employed models. It is clearly observed that the model 1 overestimates the solid volumetric fraction, showing significant errors in relation to the experimental data in all riser cross-section extension, except for the point closest to the right wall. This model also presents two maximum points of the mean time solid fraction near each riser wall. This behavior contradicts the experimental data and the results obtained with the models 2 (hybrid) and 3 (KTGF solving a PDE), respectively; and seems to be

physically incoherent.

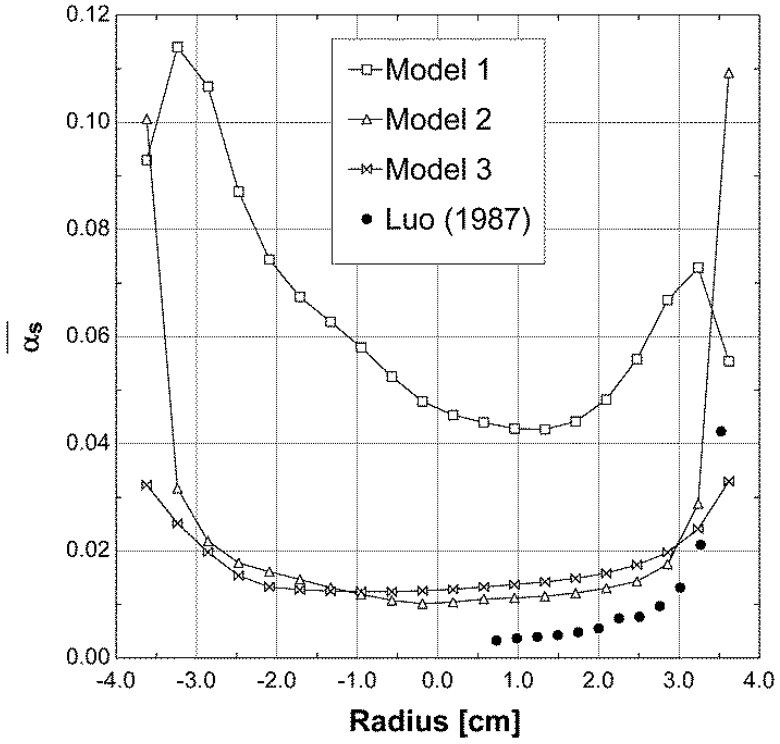

Figure 1: Radial profiles of the mean time solid volumetric fraction, 3.4 meters from the riser inlet for the models 1, 2 and 3.

It is estimated that this behavior is caused by the use of granular temperature values computed through a simplified methodology, which seems to affect considerable the computed solid pressure and viscosity quantities. In Cabezas-Gómez and Milioli (2005) is showed that the solid pressure gradient computation have a considerable influence in the numerical solution of balance equations for a gas-solid flow in a riser. The authors tested various empirical correlations for the computation of the solid pressure gradient in the context of the traditional model. Even so, if the use of empirical correlations for the constitutive relations computation is limited to their validity, it can be observed that when they are used correctly, i.e., inside their valid range, the simulation results demonstrate an adequate and qualitatively physical correct behavior. The works of Tsuo and Gidaspow (1990), Sun and Gidaspow (1999), Cabezas-Gómez and Milioli (2003) and Cabezas-Gómez et al (2008) show the validity of this affirmation. Nevertheless, only three-dimensional simulations can elucidate better up to what extend the model 1 can be used for simulating gas-solid flows in circulating fluidized bed. More research and simulations are needed in this direction. The results obtained with the models 2 and 3 displayed in Fig. 1 also show the validity of the previous discussion.

In fact, the model 2 results are those that present the better behavior in relation to the considered experimental data in the central region of the riser; and the model 3 results are those that present the better behavior in the regions near the riser walls. Even so if in the model 2 is used the same approach considered in the model 1 to compute the granular temperature, the solid pressure is calculated as in the traditional model by the correlation of Gidaspow and Ettehadieh (1983) (see Eqs. 28 and 29). This fact shows that the computation of the solid pressure is very important to obtain good enough simulation results. In this case it is seem that the use of an empirical correlation is better to compute the solid pressure instead the use of the algebraic version of the KTGF. However, when comparing with model 3 results' the same cannot be affirmed. This more complete KTGF model (model 3) leads to profiles comparable to model 2 at the riser centerline and much more appropriate in the regions near the riser walls regarding the experimental data. In this case the solid pressure computation includes the consideration of both kinetic and collisional terms, contrary to the models 1 and 2, where it is considered only collisional mechanism. Considering the results from Fig. 1 it is observed that in the central riser region all models overestimate the solid volumetric fraction in relation to the expected profiles from the experimental data.

The radial profiles of the mean time axial velocity for gas and solid phases 3.4 meters above the riser inlet are shown in Figs. 2 and 3, respectively.

In both figures the model 1 presents velocity profiles with high distortions characterizing an ascending solid flow at the right wall and a descending flow of solids at the left wall of the riser in terms of mean time variables.

This kind of flow it is not typical of CFB installations, indicating that the use of the model 1 may be not adequate to simulate the fluid dynamics of a CFB riser flow. Even if three-dimensional simulation should be performed to clearly demonstrate this affirmation, the present results are a strong indication about the model 1 weakness for simulating this type of flow.

In the case of the models 2 and 3, respectively, it is observed in Fig. 2 that model 2 leads to better results in the central riser region, while the model 3 leads to better results at the riser wall regions. The model 2 near the walls even presents negative velocity values. Considering the solid volumetric radial profiles displayed in Fig. 1, it is noted that the radial solid velocity profile is physically coherent. As the model 2 lead to a more dilute solid phase at the riser center line than the model 3, the particles in this case have a higher velocity. At the walls this behavior inverts, leading the model 2 in this region, too much more solid concentration having thus negative solid phase velocity values.

Analyzing the radial profiles of the gas velocity in Fig. 3 provided by these two models it is observed that in this case the model 3 leads to very good simulation results, presenting very small errors with the experimental data, in relation to the predictions of the models 1 and 2, respectively.

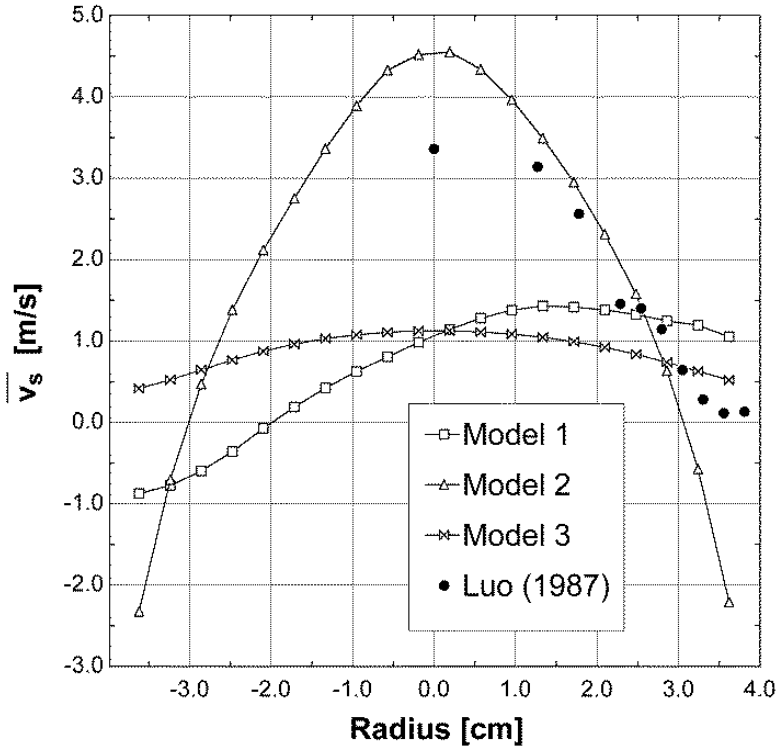

Figure 2: Radial profiles of the mean time axial solid velocity, 3.4 meters above the riser inlet considering models 1, 2 and 3, respectively.

The model 2 causes a similar behavior of that presented in Fig. 2, producing negative axial gas velocity values at the walls. These gas velocities values at the walls are caused by the high solid concentration computed by the model 2 in these regions, near riser walls. In this case the gas phase is forced to flow down near the walls by the solid phase action trough the drag force at the gas-solid interface, as a consequence of the solid phase concentration overestimation by the model.

From results showed in Fig. 3 it is clear that a more advance KTGF model should be used for simulation of riser's gas-solid flows. Future simulations should be performed considering more refined meshes at the walls, as well as, considering different boundary conditions to elucidate better how different physical models behave.

The mean time solid mass flux rate radial profiles at 5.3 meters above the riser inlet are shown in Fig. 4.

In this figure is noted that all three models present a similar behavior, showing solid mass flux negative values at the riser walls with higher in module values at the left wall. Though this behavior is not exhibited by the experimental data of Luo (1987), it is estimated that the solid mass flow at the riser exit should be higher in module at the walls where the mean time solid volumetric fraction is higher. Observing yet that the riser exit is situated at the right wall, it is expected that

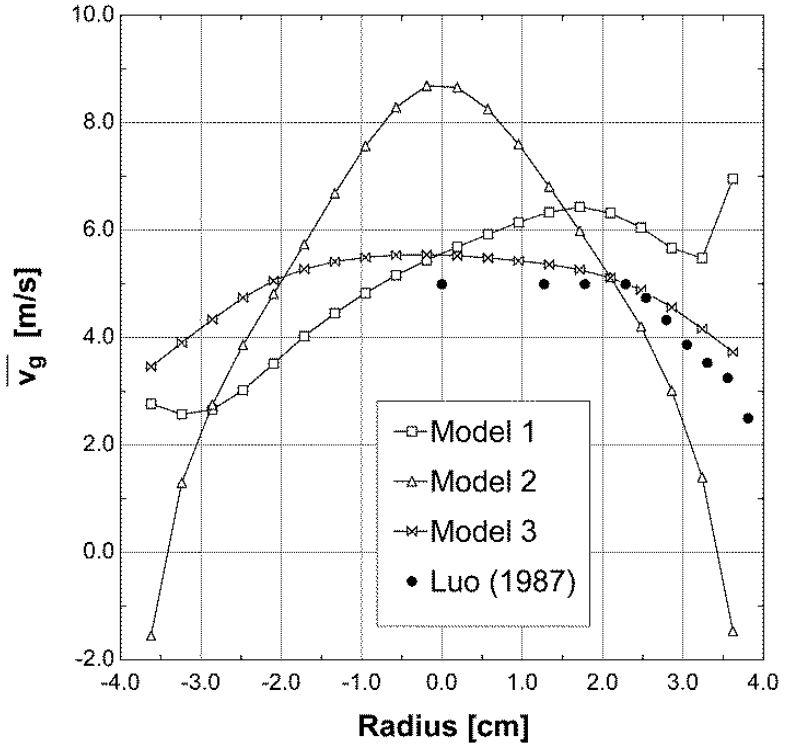

Figure 3: Radial profiles of the mean time axial gas velocity 3.4 meters above the riser inlet considering models 1, 2 and 3, respectively.

the solid phase will accumulate in the other riser side where the particles collide with the upper and lateral walls without finding an exit region. As the particles have a higher inertia than the gas phase it will be difficult to change completely their trajectory to the right wall, even if the gas phase accelerates to this direction, taking place the solid accumulations in the right riser region as showed in Fig. 4.

The experimental measurement of the solid mass flow rate is a complicated task, involving the direct measurement of the local solid volumetric fraction and the indirect measurement of the number of particles per unit of time. Even if the applied boundary conditions at the riser exit are assuming a developed flow, it is seem that the present results are physically correct. Observing in details the model 3 produces the better results in relation to the showed experimental profiles.

In Figures 5 and 6 are presented time-averaged snapshots of the gas volumetric fraction in two risers sections disposed above three and five meters height, respectively. These profiles are obtaining integrating in each computational cell the gas volumetric fraction in time (from 20 to 100 seconds).

In both figures it is observed that the models lead to different time-averaged solid concentrations, being the model 1, such that estimates the higher solid concentrations in the entire riser axial cross-section displayed in Figs. 5 and 6. These results confirm the radial solid concentration profiles displayed in Fig. 1. From

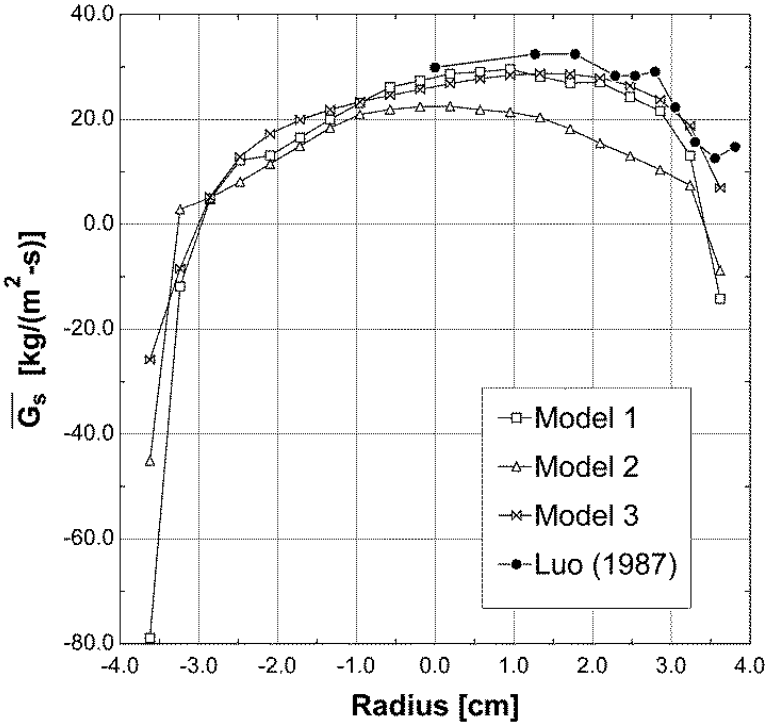

Figure 4: Radial profiles of the mean time solid mass flow rate 5.3 meters above the riser inlet considering models 1, 2 and 3, respectively.

these two figures the higher differences in the models time-averaged results are observed at section disposed near the riser exit, between 5.1 and 5.5 meters height approximately.

In this case it is observed that the model 3 leads to higher solid concentration at the upper part of the left wall, signalizing a solid concentration in this region. The models 1 and 2 prescribe some solid concentration in this region, but not so high, as that they prescribed at the lower region of this riser section. The model 1 leads to practically annular flow pattern structure, even if the analyzed riser section is near the riser outlet. This flow pattern is observed for all models in Fig. 5. This behavior is expected.

Transient snapshots of the gas volumetric fraction at the same two riser axial cross-sections are presented in Figs. 7 (above three meters height) and 8 (above five meters height) at 100 seconds of fluidization time.

These profiles are much more different than the time-averaged values, showing greatest differences across the models. The model 1 leads to high solid concentration in both figures, showing several clusters and solid accumulation in central and near walls regions. The model 2 predicts an annular flow pattern in Fig. 7 and two solid strands along the riser height and near the riser walls in Fig. 8. The model 3 predicts two visible clusters one at the right wall in Fig 7 and other less dense at the left wall in Fig. 8. This model, also produces more disperse vertical

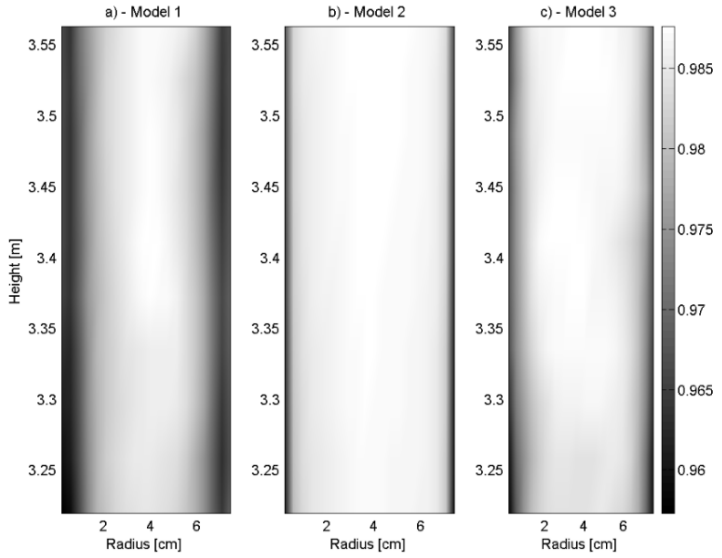

Figure 5: Time averaged snapshots of gas volumetric fraction in a riser section at three meters height approximately. a) Model 1, b) Model 2, c) Model 3.

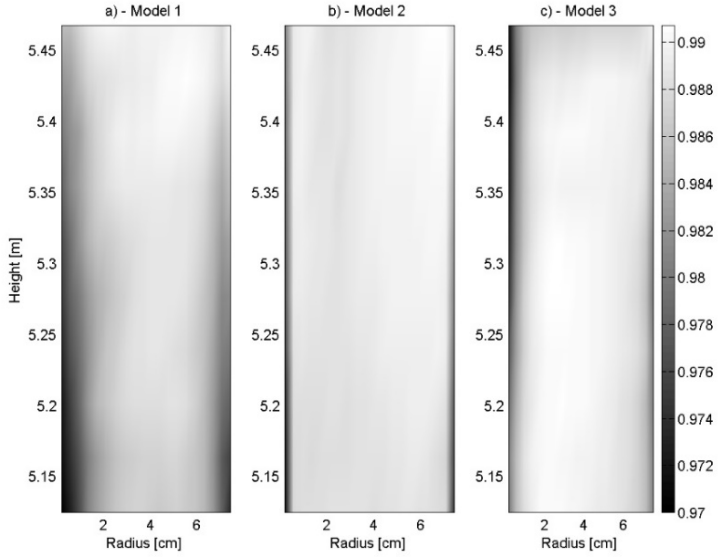

Figure 6: Time averaged snapshots of gas volumetric fraction in a riser section at five meters height approximately. a) Model 1, b) Model 2, c) Model 3.

strands in the riser central region in both figures.

These differences point to the fact that the formulation of solid constitutive equations considerable influences the gas-solid flow transient behavior, leading to quantitatively different results. Transient hydrodynamics phenomena influence in a great extent heat and chemical transport processes and consequently overall reactors parameters as performance and yield. Thus, it is important to study how

the models behave with time and what are their predictions.

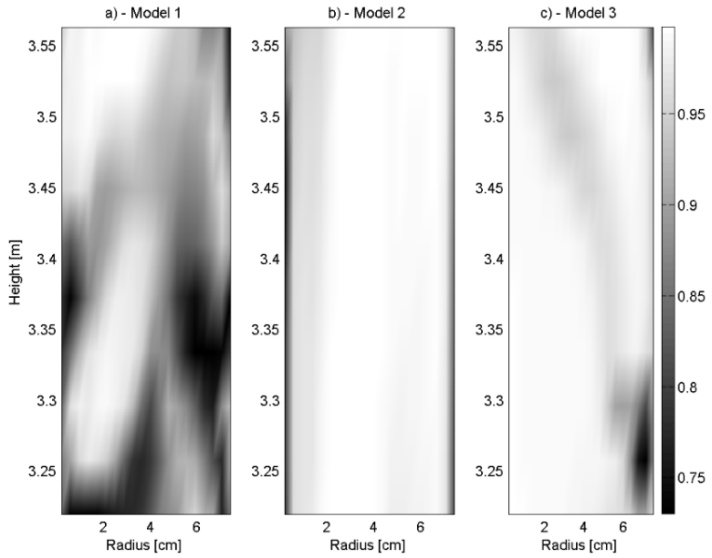

Figure 7: Temporal snapshots of gas volumetric fraction in a riser section at three meters height approximately, computed at 100 seconds of fluidization. a) - Model 1, b) - Model 2, c) - Model 3.

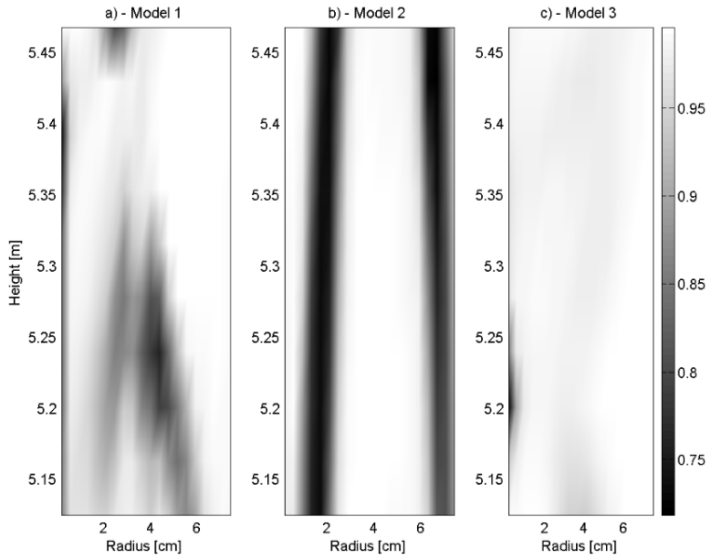

Figure 8: Temporal snapshots of gas volumetric fraction in a riser section at five meters height approximately computed at 100 seconds of fluidization. (a-) Model 1, b-) Model 2, c-) Model 3)

5 Conclusions

Considering the present numerical results can be concluded that the algebraic version of the KTGF model is not very appropriate to simulate the gas-solid flow in a CFB riser, possibly leading to non representative results of the riser hydrodynamics. One solution to this problem is the use of KTGF which solves the full partial differential equation for the granular temperature computation considering all the physical phenomena influencing the balance of the particle fluctuation velocity kinetic energy (model 3), as can be seen from the numerical results showed in section 4. With base on the present analysis it is recommended the use of the traditional algebraic KTGF for the simulation of the gas-solid flows in other installations, where the solid volumetric fraction is higher and the solid velocity is relatively small, i.e., where the granular energy is locally dissipated. The development of more complex CFB riser simulations should help to definitively establish the present conclusion, considering the numerical study of gas-solid flows in other CFB installations.

Other solution to the above problem is the use of the "ad-hoc" hybrid model proposed in the present paper. This KTGF variant has an advantage of a low computational cost of the traditional algebraic KTGF and allows obtaining satisfactory results of simulation. A positive aspect of the proposed hybrid model associated to its low computational cost is that it allows testing the many theoretical and even empirical relations existing in the literature to compute the constitutive relations for the solid phase. As expected, new investigations of the proposed model are necessary, mainly those associated with model tests through the simulations of a gas-solid flow in other CFB installations from bibliography to verify the efficiency and possibilities of this proposed model.

The complete KTGF model (model 3) was that which presented the better numerical results regarding the experimental data and it is highly recommended for simulating gas-solid riser flows. It is possible to include more physical mechanisms in the MFIX software (see Benyahia et al. (2005) and Benyahia et al. (2006))). The present model 3 considers a KTGF including the interstitial fluid effects and was extensively studied in Agrawal et al. (2001). This model is very useful for simulating gas-solid flows in CFB systems. Recent works derived from Agrawal et al. (2001), that consider the turbulent scales and a much refined scales are used extensively for CFB simulations (Sarkar et al., 2016).

6 Acknowledgments

The numerical simulations were developed with the MFIX code from the NETL (National Energy Technology Laboratory - www.mfix.org). The authors fully ap-

preciate the code availability and the support received from the researchers that develop the MFIX code.

References

Agrawal, K., Loezos, P.N., Syamlal, M., and Sundaresan, S., (2001), The role of meso-scale structures in rapid gas-solid flows, *Journal of Fluid Mechanics*, 445:151-185.

Anderson, T., and Jackson, R., (1967), A fluid mechanical description of fluidized beds, *Industrial and Engineering Chemistry Fundamentals*, 6:527-534.

Bagnold, R.A., (1954), Experiments on a Gravity-Free Dispersion of Large Solid Spheres in a Newtonian Fluid under Shear, *Proceedings of Royal Society*, A225:49-63.

Benyahia, S., Arastoopour, H., Knowlton, T.M., and Massah, H., (2000), Simulation of particles and gas flow behavior in the riser section of a circulating fluidized bed using the kinetic theory approach for the particulate phase, *Powder Technology*, 112:24-33.

Benyahia, S., Syamlal, M., and O'Brien, T.J., (2005), Evaluation of boundary conditions used to model dilute, turbulent gas/solids flows in a pipe, *Powder Technology*, 156:62-72.

Benyahia, S., Syamlal, M., and O'Brien, T.J., (2006a), Extension of Hill-Koch-Ladd drag correlation over all ranges of Reynolds number and solids volume fraction, *Powder Technology*, 162:166-174.

Benyahia, S., Syamlal, M., and O'Brien, T.J., (2006b), Summary of MFIX Equations 2005-4, from URL http://www.mfix.org/documents/MfixEquations2005-4.pdf, January, 2006.

Boemer, A., Qi, H., Renz, U., Vasquez, S., and Boysan, F., (1995), Eulerian computation of fluidized bed hydrodynamics - A comparison of physical models, *Proceedings of the 13th International Conference on Fluidized Bed Combustion*, 2:775-787.

Cabezas-Gómez, L., and Milioli, F.E., (2003), Numerical Study on the Influence of Various Physical Parameters over the Gas-solid Two-phase Flow in the 2D Riser of a Circulating Fluidized Bed, *Powder Technology*, 132:216-225.

Cabezas-Gómez, L., and Milioli, F.E., (2005), Colisional solid pressure impact on numerical results from a traditional two-fluid model, *Powder Technology*, 149:78-83.

Cabezas-Gómez, L., Silva, R.C., and Milioli, F.E., (2006), Some modeling and numerical aspects in the two-fluid simulation of the gas-solids flow in a CFB riser, *Brazilian Journal of Chemical Engineering*, 23(4):487-496.

Cabezas-Gómez, L., Silva, R.C., Navarro, H.A., and Milioli, F.E., (2008), Cluster identification and characterization in the riser of a circulating fluidized bed from numerical simulation results, *Applied Mathematical Modeling*, 32(3):327-340.

Carnahan, N.F., and Starling, K.E., (1969), Equations of state for non-attracting rigid spheres, *Journal of Chemical Physics*, 51:635-636.

Caserta, A.J., Navarro, H.A., Cabezas-Gómez, L., (2016), Damping coefficient and contact duration relations for continuous nonlinear spring-dashpot contact model in DEM, *Powder Technology*, 302:462-479.

Chapman, S., and Cowling, T.G., (1961 and 1970), The mathematical theory of non-uniform gases, 2nd 3rd Ed., *Cambrige University Press*, Cambrige, U.K.

Ding, J., and Gidaspow, D., (1990), A bubbling model using kinetic theory of granular flow, *AIChE Journal*, 36(4):523-538.

Drew, D.A., (1983), Mathematical Modeling of Two-phase Flow, *Annual Review of Fluid Mechanics*, 15:261.

Enwald, H., Peirano, E, and Almstedt, A.-E., (1996), Eulerian two-phase flow theory applied to fluidization, *International Journal of Multiphase Flow*, 22:21-66, Supplement.

Ergun, S., (1952), Fluid Flow through Packed Columns, *Chemical Engineering Progress*, 48(2):89-94.

Gera, D., Syamlal, M., and O'Brien, T.J., (2004), Hydrodynamics of particle segregation in fluidized beds, *International J. of Multiphase Flow*, 30:419-428.

Gidaspow, D., (1994), Multiphase flow and fluidization: continuum and kinetic theory descriptions, *Academic Press Inc.*, Bostom.

Gidaspow, D., and Ettehadieh, B., (1983), Fluidization in two-dimensional beds with a jet: 2. Hydrodynamic modeling, *Industrial Engineering Chemistry Research*, 22(2):193-201.

Guenther, C., and Syamlal, M., (2001), The effect of numerical diffusion on simulation of isolated bubbles in a gas-solid fluidized bed, *Powder Technology*, 116:142-154.

Huilin, L., and Gidaspow, D., (2003), Hydrodynamic Simulations of Gas-Solid Flow in a Riser, *Industrial Engng. Chemistry Research*, 42:2390-2398.

Jenike, A.W., (1987), A theory of flow of particulate solids in converging and diverging channels based on a conical yield function, *Powder Technology*, 50:229-236.

Jenkins, J.T., and Richman, M.W., (1985), Grad's 13 moment system for a dense gas of inelastic spheres, *Arch of Rational Mechanics Anal*, 87:355-377.

Jenkins, J.T., and Savage, S.B., (1983), A theory for the rapid flow of identical, smooth, nearly elastic, spherical particles, *Journal of Fluid Mechanics*, 130:187-202.

Johnson, P.C., and Jackson, R. (1987), Frictional-collisional constitutive relations for granular materials, with applications to plane shearing, *Journal of Fluid Mechanics*, 130:187-202.

Kim, H.S., and Arastoopour, H., (1995), Simulation of FCC particles flow behavior in a CFB using modified kinetic theory, *Canadian Journal of Chemical Engineers*, 73:603-611.

Lun, C.K.K., Savage, S.B., Jeffrey, D.J., and Chepurniy, N., (1984), Kinetic theories for granular flow: inelastic particles in Couette flow and slightly inelastic particles in a general flow field, *Journal of Fluid Mechanics*, 140:223-256.

Luo, K.M., Dilute, (1987), Dense-Phase and Maximum Solids-Gas Transport, *Ph.D. Thesis, Illinois Institute of Technology*, Chicago.

Neri, A., and Gidaspow, D. (2000), Riser hydrodynamic: simulation using kinetic theory, *AIChE Journal*, 46(1):52-67.

Peirano, E., (1998), Modelling and simulation of turbulent gas-solid flows applied to fluidization, *PhD. Thesis, Department of Energy Conversion, Chalmers University of Technology*, Sweden.

Sarkar, A., Milioli, F.E., Ozarkar, S., Li, T., Sun, X., Sundaresan, S., (2016), Filtered sub-grid constitutive models for fluidized gas-particle flows constructed from 3-D simulations, *Chemical Engineering Science*, 152:443-456.

Savage, S.B., (1983), Granular Flows at High Shear Rates, *In: MEYER, R.E., ed. Theory of Dispersed Multiphase Flow* New York, Academic Press, 339-358.

Schaeffer, D.G., (1987), Instability in the evolution equations describing incompressible granular flow, *Journal of Differential Equations*, 66(1):19-50.

Sinclair, J.L., and Jackson, R., (1989), Gas-solid flows in a vertical pipe with particle-particle interactions, *AIChE Journal*, 35(9):1473-1486.

Soo, S.L., (1967), Fluid Dynamics of Multiphase System, *Blaisdell Inc.*, Massachusetts.

Sun, B., and Gidaspow, D. (1999), Computation of circulating fluidized bed riser flow for the fluidization VIII benchmark test, *Industrial Engineering Chemical Research*, 38:787-792.

Sweby, P., (1984), High resolution schemes using flux limiters for hyperbolic conservation laws, *SIAM J. Numer. Anal.*, 21:995-1011.

Syamlal, M., and O'Brien, J.T., (2003), Fluid dynamic simulation of O_3 decomposition in a bubbling fluidized bed, *AIChE Journal*, 49(11):2793-2801.

Syamlal, M., Rogers, W., and O'Brien T.J., (1993), MFIX Documentation Theory Guide, *U.S. Department of Energy, Morgantown Energy Technology Center*, Technical Note DOE/MET-94/1004.

Tsuo, Y.P., and Gidaspow, D. (1990), Computation of flow patterns in circulating fluidized beds, *AIChE Journal*, 36(6):885-896.

van Wachem, B.G.M., Schouten, J.C., Krishna, R., and van den Bleek, C.M., (1998), Eulerian Simulations of Bubbling Behavior in Gas-Solid Fluidized Beds,

Computers Chemical Engineering, 22:S299-S306. Supplement.

Wen, C.Y., and Yu, Y.H., (1966), Mechanics of Fluidization, *Chemical Engineering Progress Symposium Series*, 62(62):100-111.